PART Ⅰ

Visualization of subclinical synovitis in rheumatoid arthritis

CHAPTER 2

Present role of positron emission tomography in the diagnosis and monitoring of peripheral inflammatory arthritis: a systematic review

S.T.G. Bruijnen

Y.Y.J. Gent

A.E. Voskuyl

O.S. Hoekstra

C.J. van der Laken

Arthritis Care Res 2014;66:120-30

ABSTRACT

Objective: To determine the current status of positron emission tomography (PET) as a tool for diagnosis and monitoring of peripheral inflammatory arthritis (IA).

Methods: For conducting this systematic review, the PubMed (Medline), Embase, and Cochrane Library databases were searched until December 31, 2012. Studies of PET for diagnosis and/or therapy monitoring of peripheral IA were included. Data were summarized qualitatively using best evidence synthesis.

Results: Eighteen articles met our inclusion criteria. The majority of studies were feasibility studies with varying methods applied. All studies demonstrated that PET visualized IA with high sensitivity, corresponding to clinical assessments. PET outcome of clinically active IA also matched that of ultrasound and magnetic resonance imaging. PET differentiates from other modalities by (quantitative) imaging of molecular sites in the synovium. The first studies reporting on the potential clinical applications of PET to image subclinical synovitis in preclinical RA and during therapy have been published. The results are promising, but the number and study populations of these studies are still limited.

Conclusion: Thus far, a limited number of PET studies addressing IA imaging have been published. The PET modality seems to offer highly sensitive and potentially specific imaging of IA at the (quantitative) molecular level. Clinical application studies for early diagnostics and therapy monitoring are arising, but these topics should be further explored in future studies with larger cohorts. For integration in clinical practice, aspects such as radiation burden and cost-effectiveness should also be taken into account.

INTRODUCTION

Positron emission tomography (PET) is a sensitive, quantitative, and noninvasive imaging technique that visualizes functional tissue changes by targeting binding sites (1). PET provides molecular data as opposed to anatomic and functional data obtained by ultrasonography (US) and magnetic resonance imaging (MRI). In addition, compared with other nuclear imaging techniques such as conventional scintigraphy, a great advantage of PET is the high level of sensitivity in 3-dimensional mode and its ability to quantify tracer uptake accurately and reproducibly, enabling monitoring of disease activity and therapeutic effects (2).

PET was developed in the mid-1970s after the introduction of fluorodeoxyglucose (FDG) labeled with fluorine-18 (^{18}F-FDG) (3). Three decades later, PET-computed tomography (CT) combinations were introduced for more precise anatomic localization of the PET signal (4).^{18}F-FDG is taken up in metabolically active tissues and phosphorylation prevents the glucose from being released from the cell once it has been absorbed. ^{18}F-FDG PET is extensively used in the field of oncology for diagnosis, staging, and followup (5), but its application for rheumatologic diseases is relatively new (6).

The potential of ^{18}F-FDG PET to visualize inflammatory lesions was first noticed on oncologic PET scans revealing uptake in noncancer/benign and metabolically active lesions (7). Subsequently, increasing numbers of studies reported the feasibility to image inflammatory arthritis (IA) by PET. Advanced imaging techniques such as PET are required to fulfill the clinical needs of early diagnosis of IA and optimization of therapeutic efficacy because synovitis is not shown on conventional radiographs.

In this systematic review, the current role of PET as a tool for the diagnosis and therapy monitoring of IA is discussed. We reviewed PET studies of IA, consisting of rheumatoid arthritis (RA), juvenile idiopathic arthritis (JIA), ankylosing spondylitis (AS), psoriatic arthritis (PsA), and reactive arthritis (ReA).

MATERIALS AND METHODS

Eligibility criteria

Data for this review were extracted from the collection of primary diagnostic studies reporting the use of PET, with any kind of tracer, for the diagnosis and/or therapy monitoring of peripheral IA in patients. The review included patients with RA, JIA, AS, PsA, or ReA with active peripheral arthritis on the basis of a clinical examination. To investigate the value of PET in the early diagnosis of IA, studies with patients in pre-clinical disease stages were included as well. Review articles, case reports, animal studies, scintigraphic studies without PET, and studies of patients with forms of arthritis other than those stated above (e.g., septic arthritis and spondyloarthritis) were excluded.

Information sources and search methods

Studies were identified by searching the PubMed (Medline), Embase, and Cochrane Library databases (trials) up to December 31, 2012. The search strategies for the different databases are shown in Supplementary Appendix A (available in the online version of this article at http://onlinelibrary.wiley.com/doi/10.1002/acr.22184/abstract). Because PET research in rheumatology is a relatively new topic, we performed a broad search on PET (imaging technique) in IA (disease group) without narrowing the search by a (third) outcome measure (like diagnosis or therapy monitoring). In line with this, no limits were applied for the year of publication and language (to avoid initial publication bias). Related terms in the articles and reference lists of retrieved articles were searched as well.

Study selection

Two authors (STGB and YYJG) independently screened the titles, keywords, and abstracts of retrieved studies for relevance. After consensus, the full-text versions of studies that met the eligibility criteria and of studies for which eligibility could not be determined from initial screening of the title and/or abstract were acquired. After independently assessing the full-text articles, the final inclusion was determined by consensus. In the case of disagreement, 2 authors (AEV and CJvdL) were consulted for a final decision.

Data extraction and quality assessment

To achieve uniformity, we developed 4 data extraction sheets for the 1) study population characteristics, 2) imaging characteristics (see Supplementary Appendix B, available in the online version of this article at http://onlinelibrary.wiley.com/doi/10.1002/acr.22184/abstract), 3) study outcomes, and 4) therapy monitoring characteristics. One reviewer (STGB) extracted the data from the included studies, independently controlled by a second reviewer (YYJG).

RESULTS

Study selection and inclusion

The initial search of the Pubmed (Medline), Embase, and Cochrane Library databases retrieved 2,412 articles referring to PET research in IA. Figure 1 shows the methods resulting in a final inclusion of 18 original articles.

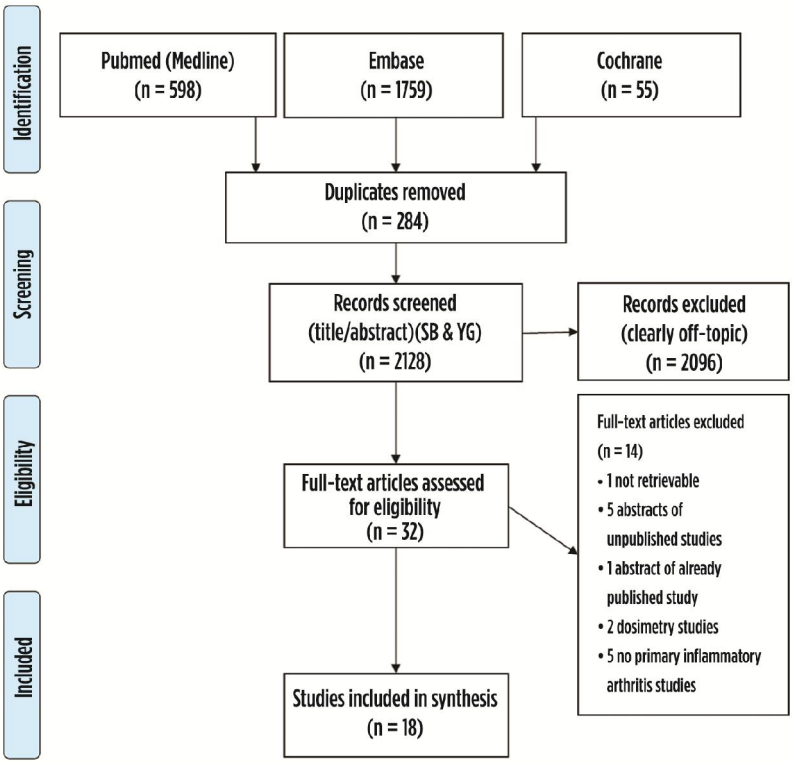

Figure 1. Flowchart of literature selection. Adapted, with permission, from ref. 53. For more information, visit www.prisma-statement.org.

Study characteristics

All assessed articles were published in English. From the first study onward (1995), in total, 18 studies including a total of 276 IA patients (175 females, 65 males, and 36 unknown) predominantly diagnosed with RA (79%) according to the American College of Rheumatology 1987 criteria were performed (8) (Tables 1- 4).

The research questions comprised the feasibility of PET to assess the disease activity of IA (n = 8), therapy monitoring (n = 9), and detection of preclinical disease activity (n = 1). PET was the only imaging modality in 6 studies, and 12 studies used PET (PET-CT) next to other imaging modalities like MRI and US. Most studies used ^{18}F-FDG as the PET tracer (15 of 18).

All studies evaluated PET data visually, but most studies also included a semiquantitative analysis (Tables 1-4). For visual assessment, a PET scan was classified as positive if tracer uptake was present in at least 1 joint. Semi-quantitative tracer uptake is usually reported as the standardized uptake value (SUV) (9), representing the ratio of tissue radioactivity concentration (measured from the PET scan) to the injected dose typically normalized for body weight (or another measure of volume of distribution, e.g., lean body mass). The tissue radioactivity concentration can be shown as the mean (SUVmean) or maximum value (SUVmax) as measured within a volume or region of interest. Sometimes, other calculations are derived from SUV, like a regional uptake value (RUV) or total uptake value (TUV), defined as the SUV in fixed planar regions of interest or the sum of the SUV in individual axial images, respectively (10). Semiquantitative data can also be obtained by the calculation of joint to control ratios. Regions of interest are then drawn on joints and (fixed) background areas.

Potential of PET to visualize clinically active IA

The potential of PET to visualize arthritis has been tested in several studies of patients with clinically active IA (Table 1). Studies by Palmer *et al.* and Polisson *et al.* were the first to show that ^{18}F-FDG PET could visualize clinical arthritis by targeting glucose metabolism (in 1995). The PET images showed locally increased ^{18}F-FDG uptake in clinically inflamed wrist joints of RA patients (10,25). In addition, the semiquantitative uptake of ^{18}F-FDG (SUV) correlated with clinical evaluations like joint swelling (TUV: r =0.53, P = 00.2 and RUV: r = 0.74, $P = 1 \times 10^{-6}$) (10). This association of SUV values of ^{18}F-FDG with clinical findings in IA cohorts was confirmed by other studies including children with JIA (11-15). (Cumulative) ^{18}F-FDG joint uptake on PET also correlated with validated clinical methods for the assessment of disease activity of RA, for example, the disease activity score in 28 joints (DAS28; up to r = 0.78, P = 0.002) (11,16,26) and the Simplified Disease Activity Index (r = 0.90, P <0.0001) (27). Instead of PET scan evaluation by

quantification of the tracer uptake in joints (SUVs), more simplified PET scoring tests have also been investigated. Three studies (12,15,16) found that simple visual scoring systems based on ^{18}F-FDG joint uptake (i.e., grading 0-4 (16)) also corresponded to clinical symptoms of arthritis.

Different studies reported concordant PET uptake in >90% of clinically active joints (17,23). However, while most studies included small populations, 3 larger ^{18}F-FDG PET studies provided some detailed data to make estimations on the diagnostic performance of PET for IA imaging (11,18,19). Derived from these studies, the sensitivity for detecting IA, with clinical assessment as the reference, varied between 56% and 77%.

^{18}F-FDG PET seems to be highly specific in the discrimination of arthritic joints from healthy joints (11) (Figure 2). However, it cannot distinguish reliably between RA and osteoarthritis. In a comparative study, more joints were PET positive in RA than in osteoarthritis (29% and 6%, respectively), but at the joint level, absolute tracer uptake did not allow a distinction between the two (19). The uptake of ^{18}F-FDG in degenerative joints has also been described in other studies (28,29). Although not very specific at the joint level, at the patient level, distribution of ^{18}F-FDG uptake in different joints shown on a whole-body scan may also help to differentiate one inflammatory rheumatic disease from the other (15,20,21). For example,^{18}F-FDG uptake in RA patients has been typically observed in the synovial tissue of (sub)clinically inflamed joints, whereas in spondyloarthritis (SpA) patients, a typical tracer uptake pattern at the entheses, reflecting enthesitis, has been observed (15,20).

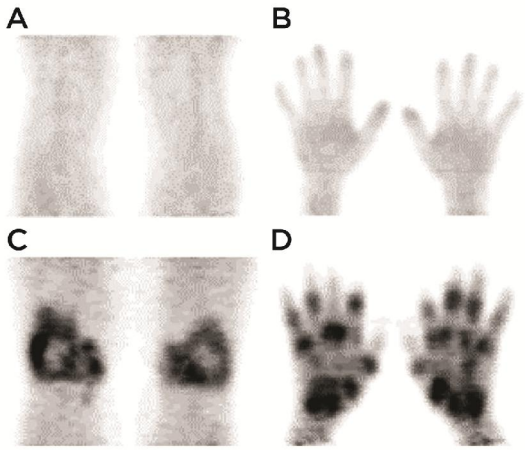

Figure 2. ^{18}F-FDG PET images of a healthy control subject and a patient with rheumatoid arthritis with active disease. A, 3-dimensional projection image of tracer distribution in a healthy knee. B, Distribution in a healthy hand and wrist. C, A rheumatoid knee. D, A rheumatoid hand and wrist. Reproduced, with permission, from ref. 11.

Radiopharmaceuticals other than ^{18}F-FDG may also be interesting for imaging IA. Danfors *et al.* found that the tracer ^{11}C-D-deprenyl accumulated in arthritic ankle joints (22). The definite mechanism underlying ^{11}C-D-deprenyl uptake in inflamed tissues has not been elucidated yet. The relationship of ^{11}C-D-deprenyl with inflammation is strengthened by the observation that corticosteroid injections block ^{11}C-D-deprenyl retention in inflammatory tissue (30).

To improve the specificity of PET tracer uptake in IA joints versus non-IA joints, specific tracers targeting molecular pathways expressed in IA synovitis are needed. A few studies have investigated the feasibility of potentially specific tracers in RA patients (see Supplementary Appendix C, available in the online version of this article at http://onlinelibrary.wiley.com/doi/10.1002/acr.22184/abstract).

Because rheumatoid synovitis is characterized by proliferative changes of synovial tissue, methyl-^{11}C-choline (choline is a precursor for synthesis of phospholipids) has been explored as a tracer (31). In 10 patients with inflammatory joint disease (among whom 2 had RA), the tracer was compared with ^{18}F-FDG (23). PET images showed fast and high accumulation of both ^{18}F-FDG and ^{11}C-choline at sites of synovitis (mean ± SD SUVs of 1.9 ± 0.9 and 1.5 ± 0.9, respectively). Although ^{11}C-choline uptake rates were 8-fold faster compared with ^{18}F-FDG (mean ± SD kinetic influx constant of 0.048 ± 0.042 minute^{-1} versus 0.006 ± 0.003 minute^{-1}), this also implied a higher chance of dependency on blood flow effects.

Another potential target to image arthritis is the macrophage, because macrophages infiltrate in synovium as RA develops and continue to play an important role in later phases. Targeting peripheral benzodiazepine receptors, particularly expressed on activated macrophages with ^{11}C-PK11195, has been successful to visualize inflammatory lesions in the brain as multiple sclerosis and vasculitis (24,32). In established RA patients with clinical arthritis of one or both knee joints, ^{11}C-(*R*)-PK11195 clearly accumulated in clinically inflamed knee joints, with mean ± SD SUV ratios of 3.2 ± 0.9, 2.3 ± 0.6, and 1.7 ± 0.4 for severe, mild, and absent clinical signs of arthritis, respectively. The SUV ratios were significantly different between groups (P <0.05). In addition, PET results highly corresponded with clinical swelling and macrophage infiltration in synovial tissue (immunohistochemistry) (24).

Table 1. Study characteristics of active IA*

Author, year (ref)	No. patients	Age, years†	Joint(s)	Tracer	PET variable	Comparative variable
Palmer et al, 1995 (10)	9 RA, 3 PsA‡	35–75	Wrist	^{18}F-FDG	RUV, TUV	Pain, tenderness, swelling
Beckers et al, 2004 (11)	21 RA‡	48 (34–69)	Knee (21 patients), wrist/MCP (13 patients), ankle/first MTP (8 patients)	^{18}F-FDG	VA, CSUV	SJC, TJC, disease duration, DAS, SDAI, PGA and phyGA
Kubota et al, 2009 (12)	18 RA‡	67 ± 11 (47–86)	Multiple (13 pp)	^{18}F-FDG	Total SUVmax, VA	Clinically positive/ negative joints, PJC, SJC
Tateishi et al, 2010 (13)	28 JIA	5.4 ± 4 (1–16)	560 joints	^{18}F-FDG	SUVmax	Swelling, tenderness, CRP level, neutrophil count, ESR, MMP-3
Okamura et al, 2012 (14)	22 RA‡	57 (20–74)	Multiple (12 pp)	^{18}F-FDG	Mean SUVmax	DAS28, DAS28-CRP, TJC, SJC, CRP level, ESR, MMP-3, RF
Vijayant et al, 2012 (15)	17 RA‡ 7 AS 3 PsA 1 nsSSA	40 (27–60) 29 (17–40) 42 (34–53) 19	Multiple (21 pp)	^{18}F-FDG	VA	Clinical diagnosis of RA, SSA, PsA
Goerres et al, 2006 (16)	7 RA‡	50 ± 18 (24–63)	Multiple (28 pp)	^{18}F-FDG	VA	DAS, RADAI
Roivainen et al, 2013 (17)	17 RA‡	51 ± 14	Multiple (54 pp)	^{18}F-FDG	VA	SJC, TJC
Beckers et al, 2006 (18)	16 RA‡	48 (34–63)	Knee	^{18}F-FDG	SUVlbm	CRP level, MMP-3, tender/swollen joints
Elzinga et al, 2007 (19)	14 RA‡ 6 OA 5 FM	57 ± 7 55 ± 11 32 ± 11	Hands and wrists	^{18}F-FDG	SUV J/C ratio	SJC, DAS Clinical diagnosis of RA, OA and FM
Taniguchi et al, 2010 (20)	7 RA 2 AS 1 PsA 1 ReA	63 ± 10 48 and 50 72 63	Multiple	^{18}F-FDG	SUVmax, VA	Clinical diagnosis of SpA and RA
Okabe et al, 2011 (21)	30 RA 2 AS	63 ± 15	Multiple (19 pp)	^{18}F-FDG	VA, SUVmax of joints	Clinical diagnosis of IA and collagen vascular disease–associated arthritis
Danfors et al, 1997 (22)	3 RA 1 JRA 1 PsA	59 24 36	Knee	^{11}C-D-deprenyl	SUV	IA and healthy controls
Roivainen et al, 2003 (23)	2 RA‡ 1 AS 6 unspecified 1 uSpA	25 and 60 48 20–48 35	Knee (9) Ankle (1)	^{18}F-FDG ^{11}C-choline	SUV, Ki	SJC, TJC
Van der Laken et al, 2008 (24)	10 RA‡	54 ± 8	Knees	^{11}C-(*R*)-PK11195	SUV J/C ratio	Semiquantitative scores of synovial swelling and PBR staining of synovial tissue

* IA = inflammatory arthritis; PET = positron emission tomography; RA = rheumatoid arthritis; PsA = psoriatic arthritis; FDG = fluorodeoxyglucose; RUV = regional uptake value defined as fixed circular regions of interest of 16 mm drawn on top of FDG uptake; TUV = total uptake value defined as the sum of standardized uptake value (SUV) in individual axial images; MCP = metacarpophalangeal; MTP = metatarsophalangeal; VA = visual assessment of tracer uptake (pattern); CSUV = cumulative SUV; SJC = swollen joint count; TJC = tender joint count; DAS = Disease Activity Score; SDAI = Simplified Disease Activity Index; PGA = patient global assessment; phyGA = physician global assessment; SUVmax = maximum SUV value; PJC = pain joint count; JIA = juvenile idiopathic arthritis; CRP = C-reactive protein; ESR = erythrocyte sedimentation rate; MMP-3 = matrix metalloproteinase 3; pp = per person; DAS28 = DAS in 28 joints; DAS28-CRP = DAS28 using the C-reactive protein level (14); RF = rheumatoid factor; SSA = seronegative spondyloarthropathy; AS = ankylosing spondylitis; nsSSA = nonspecific SSA; RADAI = Rheumatoid Arthritis Disease Activity Index; lbm = lean body mass; SUV J/C ratio = SUV from a joint divided by the SUV of a control region; OA = osteoarthritis; FM = fibromyalgia; SpA = spondyloarthritis; ReA = reactive arthritis; JRA = juvenile rheumatoid arthritis; Ki = influx constant; uSpA = undefined SpA; PBR = peripheral benzodiazepine receptor.
† Values are the mean, mean ± SD, range, mean (range), or mean ± SD (range).
* RA following the American College of Rheumatology 1987 criteria.

Comparison of PET with MRI and US in clinically active IA and treatment monitoring

Serial imaging of IA patients with PET and MRI has been reported in 4 of the included feasibility studies in clinically active RA (10,18,20,23) (Table 2). Both baseline ^{18}F-FDG uptake and pannus volume as measured with MRI, as well as their changes after treatment, correlated strongly (r = 0.86, *P* = 0.0001 and r = 0.91, *P* = 0.0002, respectively) (10,25). In line with this, uptake of both ^{11}C-choline and ^{18}F-FDG in synovium (in SUVs) corresponded with the volume of synovium on MRI, with the highest correlation coefficient for ^{11}C-choline uptake (23), suggesting that uptake of ^{11}C-choline in proliferative synovial tissue was more concordant with synovial volume on MRI than focal metabolic uptake of ^{18}F-FDG (^{18}F-FDG: r = 0.86, *P* = 0.002 and ^{11}C-choline: r = 0.95, *P* < 0.0001).

For imaging of entheses in SpA, ^{18}F-FDG PET-CT seemed to be more sensitive than MRI at lumbar spinal processes (87.5% [7 of 8] versus 50% [3 of 6]) and at ischial tuberosities (75% [6 of 8] versus 0% [0 of 5]) (20). Furthermore, ^{18}F-FDG PET results of RA patients showed correlations with US. Cumulative ^{18}F-FDG PET positivity at the group level (n = 365 joints) was significantly associated with swelling (odds ratio [OR] 4.8), tenderness (OR 8.6), and US positivity (OR 11.7) (11). Interestingly, the prevalence of ^{18}F-FDG PET-positive joints (>75%) was significantly higher than the prevalence of US-positive joints (56%). ^{18}F-FDG PET was positive in 86% of the US-positive joints and was significantly more concordant in joints with a positive power Doppler (PD) signal (i.e., PET was positive in 44 of 45 PD-positive joints [96%]). Such a signal is found in joints with hypervascularization, which is supposed to be a characteristic of active RA synovitis. The mean SUV of PD-positive joints on PET was also significantly higher than in PD-negative joints. In addition, a significant correlation between ^{18}F-FDG uptake and synovial thickness as measured by US was found for nearly all joints, except for the first metatarsophalangeal joints (all 365 joints: r = 0.56, *P* = 0.0001). This relationship was stronger for larger joints, such as the knees and ankles, than for smaller joints, such as the metacarpophalangeal joints, proximal interphalangeal joints, and wrists. This phenomenon may be explained by the technical properties of US and PET. The

detection of synovitis with US is more difficult at sites that are not easily accessible for the probe in different planes, such as the metacarpophalangeal joints (3 and 4) and the intercarpal compartments of the wrist (33,34). Besides, US does not penetrate bone. Conversely, PET has a limited spatial resolution (typically 5-6 mm) that limits the detection of small inflammatory lesions.

At present, 1 study included all 3 imaging modalities (PET, MRI, and US) in a group of IA patients (18). The results of this study showed that a positive joint on PET was significantly associated with a positive sign of arthritis on MRI and US (i.e., of the 11 PET-positive knees, 10 were also MRI positive and 10 were US positive). Moreover, in RA knee joints, changes in SUV over a period of 4 weeks of treatment also correlated with changes in MRI parameters, such as relative enhancement (r = 0.60, *P* = 0.015), rate of early enhancement (r = 0.58, *P* = 0.0177), and static enhancement (r = 0.52, *P* = 0.0396) (35), but not with changes in synovial thickness as measured with US (18).

Table 2. Study characteristics comparing PET with other imaging modalities*

Author, year (ref)	Modality	PET variable	Comparative variable
Palmer et al, 1995 (10)	PET, MRI	RUV, TUV ΔRUV, ΔTUV	MRI (VEP in mm3) ΔMRI (VEP in mm3)
Roivainen et al, 2003 (23)	PET, MRI	SUV of ^{18}F-FDG and ^{11}C-choline	MRI: volume of synovium (in cm3) and enhancement integral
Taniguchi et al, 2010 (20)	PET, MRI, Ga-67 scintigraphy	VA	MRI and Ga-67 scintigraphy
Beckers et al, 2004 (11)	PET, US	VA, CSUV	(Cumulative) synovial thickness and Doppler score on US
Beckers et al, 2006 (18)	PET, US, MRI	SUVlbm, ΔSUVlbm	US/ΔUS synovial thickness (mm) MRI/ΔMRI RE (55, 30, and 15 seconds) and SE (15 minutes)

* For the complete patient characteristics of the studies in Table 2, see Table 1. PET = positron emission tomography; MRI = magnetic resonance imaging; RUV = regional uptake value defined as fixed circular regions of interest of 16 mm drawn on top of ^{18}F-fluorodeoxyglucose (^{18}F-FDG) uptake; TUV = total uptake value defined as the sum of the standardized uptake value (SUV) in individual axial images; VEP = volume of enhancing pannus; Δ = pre- versus postintervention; Ga-67 = Gallium-67; VA = visual assessment; US = ultrasonography; CSUV = cumulative SUV; lbm = lean body mass; RE = relative enhancement; SE = static enhancement.

Subclinical IA disease activity.

The visualization of subclinical synovitis in IA patients by advanced imaging modalities has been reported in several studies (Table 3). In 2 ^{18}F-FDG PET studies, at the joint level, an average of 10% of the evaluated joints of RA patients showed signs of tracer uptake despite an absence of clinical signs of inflammation (11,19). In addition, 2 other ^{18}F-FDG PET studies reported that the cumulative and mean number PET-positive joints were (significantly) higher than the number of joints with clinical symptoms of synovitis (mean ± SD 46.4 ± 16.5 cumulative PET-positive joints and 41.7 ± 16.2 joints with clinical symptoms of synovitis [n = 7] and mean

± SD 6.2 ± 3.3 PET-positive joints and 3.1 ± 2.7 joints with clinical symptoms of synovitis [n = 17; *P* =0.0002]) (12,16). Moreover, by targeting macrophages using ^{11}C-(*R*)-PK11195 PET, the SUV ratios in 5 clinically uninflamed knee joints (mean ± SD 1.7 ± 0.4) of RA patients were significantly higher than those in uninflamed knee joints of control subjects (mean ± SD 1.1 ±0.1; *P* <0.05) (24). Interestingly, one ^{18}F-FDG PET study in RA included 4 remission patients.

Although tracer joint uptake was lower than in those patients with clinically active disease (total mean ± SD SUVmax 22.0 ± 1.8 versus 33.4 ± 12.1; *P* <0.001), all 4 remission patients had at least 1 PET-positive joint (12).

Although a false-positive PET signal in these asymptomatic joints cannot be excluded, a recent prospective study supports the relevance of such observations. All of the 4 anti-citrullinated protein antibody-positive arthralgia patients without clinical signs of arthritis with a positive^{11}C-(*R*)-PK11195 PET at baseline developed IA within 1 year of clinical followup, whereas the majority (20 of 25 patients) of those with a negative ^{11}C-(*R*)-PK11195 PET at baseline did not develop any IA in a 2-year followup period (36). Only 2 of 5 patients with a negative PET scan of the hands developed subtle arthritis in 1 or 2 hand joints while the others developed arthritis outside the field of view of the PET scan. These data support detection of subclinical IA in the very early phase of developing RA by PET and macrophage targeting (Figure 3).

Table 3. Study characteristics reporting subclinical disease activity*

Author, year (ref.)	No. patients†	Age, years	Joints	Tracer	PET variable	Comparative variable
Beckers et al, 2004 (11)	21 RA‡	48 (34-69)	21 joints (see Table 1)	^{18}F-FDG	VA	Clinical joint assessment
Elzinga et al, 2007 (19)	14 RA‡	57 ± 7	Hands and wrists	^{18}F-FDG	VA	Clinical joint assessment
Kubota et al, 2009 (12)	18 RA‡	67 ± 11 (47-86)	Multiple (13 pp)	^{18}F-FDG	SUV	Assessment of clinical remission
Goerres et al, 2006 (16)	7 RA‡	50 ± 18 (24-63)	Multiple (28 pp)	^{18}F-FDG	VA	Clinical total joint score
Van der Laken, 2008 (24)	10 RA‡	54 ± 8	Knees	^{11}C-(*R*)-PK11195	SUV ratio arthritis/ contralateral joint	RA patients and controls
Gent et al, 2012 (36)	29 ACPA 3 RA‡	44 ± 12 49 ± 10	Hands and wrists	^{11}C-(*R*)-PK11195	VA	Clinical assessment at baseline and followup

* PET = positron emission tomography; RA = rheumatoid arthritis; FDG = fluorodeoxyglucose; VA = visual assessment; pp = per person; SUV = standardized uptake value; ACPA = anti- citrullinated protein antibody-positive arthralgia patients.
† Values are the mean (range), mean ± SD, or mean ± SD (range).
* RA following the American College of Rheumatology 1987 criteria.

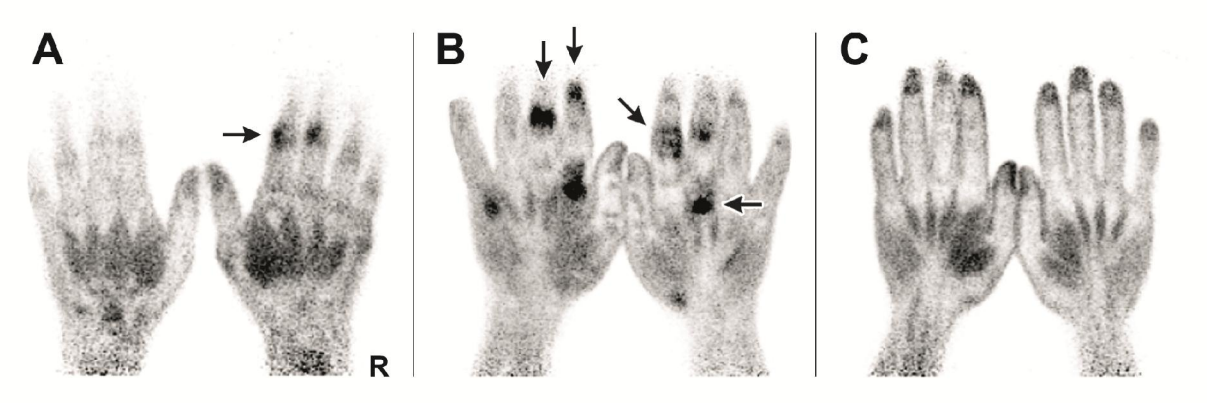

Figure 3. Representative ^{11}C-(*R*)-PK11195 images of the hands and wrists in A, an anti-citrullinated protein antibody-positive individual with arthralgia, B, a rheumatoid arthritis patient with clinical arthritis in various hand joints, and C, a healthy volunteer without joint uptake. Arrows indicate examples of joints with elevated tracer uptake. Note the background uptake of the tracer in intrinsic hand muscles and bone marrow and around the nails in all images. R = right hand. Reproduced, with permission, from ref. 36.

Treatment monitoring and prediction

The characteristics of PET to quantify tracer uptake at the molecular level potentially allow for treatment monitoring. This application has been addressed in several studies in IA (Table 4). A decline (up to 58%) of both ^{18}F-FDG and ^{11}C-D-deprenyl was noticed in arthritic joints after (antirheumatic) drug interventions (10,17,22). Furthermore, ^{18}F-FDG PET data, both quantitative and visual, were in agreement, with clinical changes of disease activity (DAS28) during anti-tumor necrosis factor treatment (14,16). In 22 RA patients, the mean ± SD of the cumulative SUVmax of 12 joints per patient significantly decreased from 2.14 ± 0.55 to 1.66 ± 0.48 (P <0.005) and the mean ± SD DAS28 score decreased significantly from 5.29 ± 1.01 to 3.81 ± 0.86 (P <0.001); these independent changes correlated significantly (r = 0.538, P = 0.01) (14). A simple visual PET scoring system for response assessment, investigated in 7 RA patients, also showed a significant correlation between a decrease of PET signal (mean ± SD 46.4 ± 16.5 to 41.7 ±16.2) and DAS28 score (mean ± SD 5.6 ± 1.2 to 3.3 ± 1.2; P = 0.04) (16). It should be noted that the determination of tracer uptake by visual assessment is less accurate than (semi)quantification of the uptake. An example of this was shown in a study by Vijayant et al; in this therapy monitoring study, the authors found that ^{18}F-FDG uptake remained visually high despite decreases in SUVmax (15).

Changes in quantitative PET data also seemed to correlate with changes in serum inflammation levels, such as C-reactive protein (CRP) after 4 weeks (r = 0.51, P = 0.004) and

12 weeks (r = 0.90, *P* = 0.002) of treatment (17,18). Conversely, in treatments with a lack of change in serum inflammation levels such as acupuncture, PET corresponded to an absence of significant SUV changes (37).

Besides treatment monitoring, PET might also allow for the prediction of treatment efficacy early in the course of treatment, or ultimately at baseline. Two studies compared ^{18}F-FDG PET data of RA patients before and a few weeks after treatment (17,38). In 16 RA patients, a significant correlation was found between early changes (0-2 weeks) of ^{18}F-FDG uptake (mean SUV) in the hands and wrists and DAS28 score at 14 weeks (r = 0.62, *P* = 0.05) and 22 weeks (r = 0.65, *P* = 0.01). In addition, in 17 RA patients, the percentage of ^{18}F-FDG PET changes of multiple joints (also including the hands and wrists) between baseline and 2 or 4 weeks corresponded with the percentage of changes of clinical disease activity (DAS28 using the erythrocyte sedimentation rate [ESR]) at 12 weeks (r =0.58, *P* = 0.014 at 2 weeks, data not available at 4 weeks) (17). In contrast, no correlation was found between changes in ESR, CRP level, and DAS28 between 0-2 weeks of treatment and clinical outcome at 14 weeks (38), suggesting that ^{18}F-FDG has a stronger prognostic value for treatment response than currently available parameters in the early phase of treatment.

Table 4. Study characteristics reporting treatment monitoring*

Author, year (ref)	No. patients	Age, years†	Joints	Tracer	PET variable	Comparative variable‡	Therapy
Palmer et al, 1995 (10)	9 RA§ 3 PsA	NA 35-75	Wrist	^{18}F-FDG	RUV, TUV	Paulus Index	NSAID (piroxicam), prednisone, MTX
Danfors et al, 1997 (22)	3 RA 1 JRA 1 PsA	59 24 36	Knee	^{11}C-D-deprenyl	ΔSUV	Clinical improvement (no detailed information available)	Steroid injections L-deprenyl, synovectomy
Goerres et al, 2006 (16)	7 RA§	50 ± 18 (24-63)	Multiple (28 pp)	^{18}F-FDG	VA (score 0-4)	EULAR response criteria	Infliximab
Vijayant et al, 2012 (15)	9 RA§	NA	Multiple (21 pp)	^{18}F-FDG	% change in SUVmax, VA	% change in TJC, SJC SUVmax	MTX, hydroxychloroquine, prednisolone
Okamura et al, 2012 (14)	22 RA§	57 (20-74)	Multiple (12 pp)	^{18}F-FDG	Δmean SUVmax, SUVmax	ΔDAS28, ΔDAS28-CRP, ΔTJC, ΔSJC, ΔCRP level, ΔESR, ΔMMP- 3, ΔRF	Etanercept, infliximab
Beckers et al, 2006 (18)	16 RA§	48 (34-63)	Knee	^{18}F-FDG	ΔSUVlbm	ΔCRP level/ ΔMMP-3	Anti-TNF*a.* therapy
Roivainen et al, 2013 (17)	17 RA§	51 ± 14	Multiple (54 pp)	^{18}F-FDG	SUV ΔSUVmax ΔSUVmax (at 2 and 4 weeks)	SJC, TJC, ESR, CRP level ΔCRP level/ΔESR ΔDAS28-ESR (at week 12)	MTX, sulfasalazine, hydroxychloroquine, prednisolone
Sato et al, 2009 (37)	6 RA§	61 ± 12 (41-75)	Knee	^{18}F-FDG	SUVmax Volume SUV >1 in cm3	VAS, ROM, face Scale for mood, M-HAQ, ESR, CRP level	Acupuncture
Elzinga et al, 2011 (38)	16 RA§	53 ± 10	MCP and wrists	^{18}F-FDG	Δmean SUV (0-2 weeks)	DAS 14 weeks/ 22 weeks	Infliximab

* PET = positron emission tomography; RA = rheumatoid arthritis; NA = not available; FDG = fluorodeoxyglucose; RUV = regional uptake value defined as fixed circular regions of interest of 16 mm drawn on top of 18F-FDG uptake; TUV = total uptake value defined as the sum of standardized uptake value (SUV) in individual axial images; Paulus Index = analysis of treatment response (39); NSAID = nonsteroidal antiinflammatory drug; MTX = methotrexate; PsA = psoriatic arthritis; Δ = pre- versus postintervention; JRA = juvenile rheumatoid arthritis; pp = per person; VA = visual assessment; EULAR = European League Against Rheumatism; SUVmax = maximum SUV value; TJC = tender joint count; SJC = swollen joint count; DAS28 = Disease Activity Score in 28 joints; DAS28-CRP = DAS28 using the C-reactive protein level (14); ESR = erythrocyte sedimentation rate; MMP-3 = matrix metalloproteinase 3; RF = rheumatoid factor; lbm = lean body mass; anti-TNF*a.* = anti-tumor necrosis factor *a.*; DAS28-ESR = DAS28 using the ESR; VAS = visual analog scale; ROM = range of motion; M-HAQ = modified Health Assessment Questionnaire; MCP = metacarpophalangeal.
† Values are the mean, range, mean (range), mean ± SD, or mean ± SD (range).
* Most patients were investigated within 1 week of physical examination for clinical response assessment.
§ RA following the American College of Rheumatology 1987 criteria.

DISCUSSION

This review included 18 primary studies that reported the results of PET research in patients with peripheral IA, primarily RA. The proof of concept of sensitive semiquantitative imaging of IA by PET was demonstrated in these studies. Because of high costs and radiation burden, PET will not be useful in clinical practice for the imaging of clinically active IA that can be easily determined by clinical assessments. However, because the spectrum of IA is changing toward diagnosis in the preclinical phase of disease, advanced imaging detecting subclinical disease activity is required. Moreover, the clinical need to increase the efficacy of expensive biologic agents warrants sensitive and quantitative monitoring of therapy. PET studies that address these needs are now arising. The first results of such studies are promising and may suggest a role for PET in early diagnostics and for monitoring or ultimately the prediction of therapeutic efficacy, eventually contributing to individualized therapy. Likewise, PET has already been implemented in the clinical practice of oncology for the diagnosis, staging, and therapy monitoring of the disease (5). Finally, positive correlations between simple visual PET scoring and clinical assessments may enhance implementation of PET analysis in clinical practice.

Although the yield of information derived from this review is valuable, this review has its limitations. The number of PET studies investigating imaging of peripheral IA is still limited. Most studies had a proof-of-concept design focused on the feasibility of imaging of clinically active IA (mostly focused on RA) with small sample sizes and great heterogeneity in study design, patient selection, and analysis. The latter implies that pooling of data was not possible and consequently the results were presented in a descriptive manner.

Most PET studies in this review (15 of 18 studies) used ^{18}F-FDG as the tracer. Although this tracer performs well in the imaging of IA, it is nonspecific and accumulates in any joint that is metabolically active, as also noticed in osteoarthritis and other systemic (infection) diseases (19,40 -44). The application of specific tracers targeting different processes in the inflammatory cascade of IA (45) may contribute to increased specificity (22-24,36). Besides the application of specific tracers, *in vivo* biodistribution of the tracer (e.g., predominantly uptake in the synovium in RA versus uptake in the entheses in SpA) may also contribute to the differentiation of inflammatory joint diseases (12,20).

The advantage of the technique of PET to image and quantify pathophysiology at the molecular level as well as the option to apply specific tracers makes PET a highly sensitive and potentially specific modality for imaging subclinical IA. With the introduction of the hybrid technique PET-CT, the molecular information can be localized more precisely by using (low-dose) CT scans for anatomic delineation of the PET signal. In particular, with regard to molecular quantification and the aspect of specificity, PET may have advantages over anatomic/functional

imaging techniques such as MRI and US. These latter techniques have suboptimal quantification in a longitudinal setting (46) for the detection of subtle early or residual synovitis activity, which is relevant for early diagnostics and therapy monitoring. The other advantages of PET are whole-body imaging in 1 session within 20-30 minutes (or even shorter for particular tracers as derived from kinetic analyses) and independency of operator skills.

The disadvantages of PET are the use of radioactivity, the poor spatial resolution (and hence a major impediment to quantification), and the costs and variable availability of PET facilities. The use of radioisotopes can lead to an effective dose (47) of ~7 mSv when 370 MBq of the tracer ^{18}F-FDG is used. A low-dose whole-body attenuation CT would add ~3-5 mSv, leading to a total PET-CT effective dose of 10-12 mSv for whole-body imaging. For comparison, the mean effective dose of a diagnostic CT of the abdomen is 10 mSv (48). This radiation burden is 4-5 times the yearly natural background radiation dose according to the United Nations and is comparable with an equivalent of 500 chest radiographs (49). Exposure to radiation can be diminished by the usage of radioisotopes with a shorter half-life, which would be relevant in the case of repetitive scanning and as might be relevant for therapy monitoring.

This systematic review of mainly feasibility studies demonstrated that PET offers highly sensitive and potentially specific imaging of IA. For clinical practice, the technique may have value for the detection of early or residual subclinical synovitis. Specific tracers targeting inflammatory sites in the synovium are being developed and tested. Multicenter, large-scale validation studies with uniform, comparable outcome measures are obligatory to elucidate the definite role for PET in the early diagnosis and therapy monitoring of IA. One of the challenges is the development of standardized PET analysis methods. These studies could be performed in line with oncologic studies, for which a worldwide standardized guideline for tumor PET imaging and PET response criteria is available, allowing multicenter studies (50,51). To further determine the strengths and weaknesses of PET as a diagnostic and monitoring tool for IA in relation to other imaging modalities, comparative studies in large cohorts are warranted. Validation studies should also address cost-effectiveness. Although the costs of PET are currently still high, they may decrease in time upon an increase in the applicability of PET in clinical practice. Moreover, PET may even save costs if it can be shown that PET can delay or most optimally prevent the onset of IA and/or increase the therapeutic efficacy of expensive biologic agents.

Finally, the hybrid imaging technique PET-MRI has been recently introduced in the first medical centers to use this technique. Preliminary PET-MRI fusion images of RA patients have shown interesting results (28,52). PET-MRI combines highly sensitive functional imaging at the molecular level with superior anatomic details (including synovial tissue changes and bone

edema) without the additional radiation burden of CT. In particular, the latter aspect may increase the options for practical implementation of PET for IA imaging. PET-MRI needs to be further explored in future studies of imaging of IA.

SIGNIFICANCE & INNOVATIONS

- Positron emission tomography (PET) allows for sensitive, noninvasive imaging of inflammatory arthritis (IA) of the whole body in 1 imaging session. Specificity may be achieved by application of tracers that bind to molecular inflammatory targets in synovial tissue. PET has advantages over scintigraphy for the imaging of arthritis due to a higher sensitivity for the detection of low-grade inflammation, 3-dimensional imaging, and the potential to quantify tracer uptake.
- Because of costs and radiation burden, PET will not have clinical value for the diagnostics of clinically accessible arthritis. However, it has the potential (as indicated by recent study data) to address the clinical needs of detection of early (preclinical) IA disease activity and monitor or ultimately predict the therapeutic outcome (in particular of expensive biologic agents) through sensitive imaging of subclinical synovitis and quantification of the PET data. Studies with large cohorts, uniform scanning protocols, and comparable outcome measures are warranted to further explore and potentially validate PET for these clinical applications.
- The novel characteristics of PET in imaging at the molecular level of synovial tissue distinguish this technique from anatomic and functional techniques such as magnetic resonance imaging (MRI) and ultrasound (US). Feasibility studies have demonstrated comparable sensitivity of the different techniques to image clinically active IA. However, head-to-head comparisons of PET to MRI and/or US (or by application of hybrid imaging PET-MRI) for detection of subclinical synovitis are still lacking. Specificity may be an advantage of PET but needs to be addressed in future studies using 2 or more imaging modalities.

REFERENCES

1. Jones T. The role of positron emission tomography within the spectrum of medical imaging. Eur J Nucl Med 1996;23:207-11.
2. Tomasi G, Turkheimer F, Aboagye E. Importance of quantification for the analysis of PET data in oncology: review of current methods and trends for the future. Mol Imaging Biol 2012;14:131-46.
3. Phelps ME, Hoffman EJ, Mullani NA, Ter-Pogossian MM. Application of annihilation coincidence detection to transaxial reconstruction tomography. J Nucl Med 1975;16:210-24.
4. Beyer T, Townsend DW, Brun T, Kinahan PE, Charron M, Roddy R, et al. A combined PET/CT scanner for clinical oncology. J Nucl Med 2000;41:1369-79.
5. Gambhir SS, Czernin J, Schwimmer J, Silverman DH, Coleman RE, Phelps ME. A tabulated summary of the FDG PET literature. J Nucl Med 2001;42 Suppl:1S-93S.
6. Tan AL, Keen HI, Emery P, McGonagle D. Imaging inflamed synovial joints. Methods Mol Med 2007;135:3-26.
7. Larson SM. Cancer or inflammation? A holy grail for nuclear medicine. J Nucl Med 1994;35:1653-5.
8. Arnett FC, Edworthy SM, Bloch DA, McShane DJ, Fries JF, Cooper NS, et al. The American Rheumatism Association 1987 revised criteria for the classification of rheumatoid arthritis. Arthritis Rheum 1988;31:315-24.
9. Zasadny KR, Wahl RL. Standardized uptake values of normal tissues at PET with 2-[fluorine-18]-fluoro-2-deoxy-D-glucose:variations with body weight and a method for correction. Radiology 1993;189:847-50.
10. Palmer WE, Rosenthal DI, Schoenberg OI, Fischman AJ, Simon LS, Rubin RH, et al. Quantification of inflammation in the wrist with gadolinium-enhanced MR imaging and PET with 2-[F-18]-fluoro-2-deoxy-D-glucose. Radiology 1995;196:647-55.
11. Beckers C, Ribbens C, Andre B, Marcelis S, Kaye O, Mathy L, et al. Assessment of disease activity in rheumatoid arthritis with 18F-FDG PET. J Nucl Med 2004;45:956 - 64.
12. Kubota K, Ito K, Morooka M, Mitsumoto T, Kurihara K, Yamashita H, et al. Whole-body FDG-PET/CT on rheumatoid arthritis of large joints. Ann Nucl Med 2009;23:783-91.
13. Tateishi U, Imagawa T, Kanezawa N, Okabe T, Shizukuishi K, Inoue T, et al. PET assessment of disease activity in children with juvenile idiopathic arthritis. Pediatr Radiol 2010;40:1781-8.
14. Okamura K, Yonemoto Y, Arisaka Y, Takeuchi K, KobayashiT, Oriuchi N, et al. The assessment of biologic treatment in patients with rheumatoid arthritis using FDG-PET/CT. Rheumatology (Oxford) 2012;51:1484-91.
15. Vijayant V, Sarma M, Aurangabadkar H, Bichile L, Basu S. Potential of 18F-FDG-PET as a

valuable adjunct to clinical and response assessment in rheumatoid arthritis and seronegative spondyloarthropathies. World J Radiol 2012;4:462-8.

16. Goerres GW, Forster A, Uebelhart D, Seifert B, Treyer V, Michel B, et al. F-18 FDG whole-body PET for the assessment of disease activity in patients with rheumatoid arthritis. Clin Nucl Med 2006;31:386-90.
17. Roivainen A, Hautaniemi S, Mottonen T, Nuutila P, OikonenV, Parkkola R, et al. Correlation of 18F-FDG PET/CT assessments with disease activity and markers of inflammation inpatients with early rheumatoid arthritis following the initiation of combination therapy with triple oral antirheumatic drugs. Eur J Nucl Med Mol Imaging 2013;40:403-10.
18. Beckers C, Jeukens X, Ribbens C, Andre B, Marcelis S, Leclercq P, et al. 18F-FDG PET imaging of rheumatoid knee synovitis correlates with dynamic magnetic resonance and sonographic assessments as well as with the serum level ofmetalloproteinase-3. Eur J Nucl Med Mol Imaging 2006;33:275-80.
19. Elzinga EH, van der Laken CJ, Comans EF, Lammertsma AA, Dijkmans BA, Voskuyl AE. 2-deoxy-2-[F-18]fluoro-D-glucose joint uptake on positron emission tomography images: rheumatoid arthritis versus osteoarthritis. Mol Imaging Biol 2007; 9:357-60.
20. Taniguchi Y, Arii K, Kumon Y, Fukumoto M, Ohnishi T,Horino T, et al. Positron emission tomography/computed tomography: a clinical tool for evaluation of enthesitis in patients with spondyloarthritides. Rheumatology (Oxford) 2010;49:348-54.
21. Okabe T, Shibata H, Shizukuishi K, Yoneyama T, Inoue T, Tateishi U. F-18 FDG uptake patterns and disease activity of collagen vascular diseases-associated arthritis. Clin Nucl Med 2011;36:350-4.
22. Danfors T, Bergstrom M, Feltelius N, Ahlstrom H, Westerberg G, Langstrom B. Positron emission tomography with 11C-D-deprenyl in patients with rheumatoid arthritis: evaluation of knee joint inflammation before and after intra-articular glucocorticoid treatment. Scand J Rheumatol 1997;26:43-8.
23. Roivainen A, Parkkola R, Yli-Kerttula T, Lehikoinen P, Viljanen T, Mottonen T, et al. Use of positron emission tomography with methyl-11C-choline and 2-18F-fluoro-2-deoxy-D-glucose in comparison with magnetic resonance imaging for the assessment of inflammatory proliferation of synovium. Arthritis Rheum 2003;48:3077-84.
24. Van der Laken CJ, Elzinga EH, Kropholler MA, Molthoff CF,van der Heijden JW, Maruyama K, et al. Noninvasive imaging of macrophages in rheumatoid synovitis using 11C-(R)-PK11195 and positron emission tomography. Arthritis Rheum 2008;58:3350-5.
25. Polisson RP, Schoenberg OI, Fischman A, Rubin R, Simon LS, Rosenthal D, et al. Use of magnetic resonance imaging and positron emission tomography in the assessment of

synovial volume and glucose metabolism in patients with rheumatoid arthritis. Arthritis Rheum 1995;38:819-25.

26. Prevoo ML, van 't Hof MA, Kuper HH, van Leeuwen MA, van de Putte LB, van Riel PL. Modified disease activity scores that include twenty-eight-joint counts: development and validation in a prospective longitudinal study of patients with rheumatoid arthritis. Arthritis Rheum 1995;38:44-8.
27. Smolen JS, Breedveld FC, Schiff MH, Kalden JR, Emery P,Eberl G, et al. A simplified disease activity index for rheumatoid arthritis for use in clinical practice. Rheumatology (Oxford) 2003;42:244-57.
28. Chaudhari AJ, Bowen SL, Burkett GW, Packard NJ, Godinez F, Joshi AA, et al. High-resolution 18F-FDG PET with MRI for monitoring response to treatment in rheumatoid arthritis. Eur J Nucl Med Mol Imaging 2010;37:1047.
29. Kalicke T, Schmitz A, Risse JH, Arens S, Keller E, Hansis M,et al. Fluorine-18 fluorodeoxyglucose PET in infectious bone diseases: results of histologically confirmed cases. Eur J Nucl Med 2000;27:524-8.
30. Linnman C, Appel L, Fredrikson M, Gordh T, Soderlund A, Langstrom B, et al. Elevated [11C]-D-deprenyl uptake in chronic whiplash associated disorder suggests persistent musculoskeletal inflammation. PLoS One 2011;6:e19182.
31. Wunder A, Straub RH, Gay S, Funk J, Muller-Ladner U. Molecular imaging: novel tools in visualizing rheumatoid arthritis. Rheumatology (Oxford) 2005;44:1341-9.
32. Lamare F, Hinz R, Gaemperli O, Pugliese F, Mason JC, Spinks T, et al. Detection and quantification of large-vessel inflammation with 11C-(R)-PK11195 PET/CT. J Nucl Med 2011;52:33-9.
33. Baillet A, Gaujoux-Viala C, Mouterde G, Pham T, Tebib J, Saraux A, et al. Comparison of the efficacy of sonography, magnetic resonance imaging and conventional radiography for the detection of bone erosions in rheumatoid arthritis patients: a systematic review and meta-analysis. Rheumatology (Oxford) 2011;50:1137-47.
34. Szkudlarek M, Court-Payen M, Jacobsen S, Klarlund M, Thomsen HS, Ostergaard M. Interobserver agreement in ultrasonography of the finger and toe joints in rheumatoid arthritis. Arthritis Rheum 2003;48:955-62.
35. Ostergaard M, Lorenzen I, Henriksen O. Dynamic gadolinium-enhanced MR imaging in active and inactive immunoinflammatory gonarthritis. Acta Radiol 1994;35:275-81.
36. Gent YY, Voskuyl AE, Kloet RW, van Schaardenburg D, Hoekstra OS, Dijkmans BA, et al. Macrophage positron emission tomography imaging as a biomarker for preclinical rheumatoid arthritis: findings of a prospective pilot study. Arthritis Rheum 2012;64:62-6.

37. Sato M, Inubushi M, Shiga T, Hirata K, Okamoto S, Kamibayashi T, et al. Therapeutic effects of acupuncture in patients with rheumatoid arthritis: a prospective study using 18F-FDG-PET. Ann Nucl Med 2009;23:311-6.
38. Elzinga EH, van der Laken CJ, Comans EF, Boellaard R, Hoekstra OS, Dijkmans BA, et al. 18F-FDG PET as a tool to predict the clinical outcome of infliximab treatment of rheumatoid arthritis: an explorative study. J Nucl Med 2011;52:77-80.
39. Paulus HE, Egger MJ, Ward JR, Williams HJ, and the Cooperative Systematic Studies of Rheumatic Diseases Group. Analysis of improvement in individual rheumatoid arthritis patients treated with disease-modifying antirheumatic drugs, based on the findings in patients treated with placebo. Arthritis Rheum 1990;33:477-84.
40. Duet M, Pouchot J, Liote F, Faraggi M. Role for positron emission tomography in skeletal diseases. Joint Bone Spine 2007;74:14-23.
41. Dumarey N, Egrise D, Blocklet D, Stallenberg B, Remmelink M, del Marnol V, et al. Imaging infection with 18F-FDG-labeled leukocyte PET/CT: initial experience in 21 patients. J Nucl Med 2006;47:625-32.
42. Kumar R, Basu S, Torigian D, Anand V, Zhuang H, Alavi A. Role of modern imaging techniques for diagnosis of infection in the era of 18F-fluorodeoxyglucose positron emission tomography. Clin Microbiol Rev 2008;21:209-24.
43. Sugawara Y, Braun DK, Kison PV, Russo JE, Zasadny KR, Wahl RL. Rapid detection of human infections with fluorine-18 fluorodeoxyglucose and positron emission tomography:preliminary results. Eur J Nucl Med 1998;25:1238-43.
44. Zhuang H, Yu JQ, Alavi A. Applications of fluorodeoxyglucose-PET imaging in the detection of infection and inflammation and other benign disorders. Radiol Clin North Am 2005;43:121-34.
45. Dorward DA, Lucas CD, Rossi AG, Haslett C, Dhaliwal K. Imaging inflammation: molecular strategies to visualize key components of the inflammatory cascade, from initiation to resolution. Pharmacol Ther 2012;135:182-99.
46. Gu JT, Nguyen L, Chaudhari AJ, Mackenzie JD. Molecular characterization of rheumatoid arthritis with magnetic resonance imaging. Top Magn Reson Imaging 2011;22:61-9.
47. Rosenstein M. Diagnostic reference levels for medical exposure of patients: ICRP guidance and related ICRU quantities. Health Phys 2008;95:528-34.
48. Picano E. Sustainability of medical imaging. BMJ 2004;328:578-80.
49. UNSCEAR 2010 report. 2011. URL: http://www.unscear.org/docs/reports/2010/UNSCEAR_2010_Report_M.pdf.
50. Boellaard R, O'Doherty MJ, Weber WA, Mottaghy FM, Lonsdale MN, Stroobants SG, et al.

FDG PET and PET/CT: EANM procedure guidelines for tumour PET imaging. Version1.0. Eur J Nucl Med Mol Imaging 2010;37:181-200.

51. Wahl RL, Jacene H, Kasamon Y, Lodge MA. From RECIST to PERCIST: evolving considerations for PET response criteria in solid tumors. J Nucl Med 2009;50 Suppl 1:122S-50S.
52. Miese F, Scherer A, Ostendorf B, Heinzel A, Lanzman RS, Kropil P, et al. Hybrid 18F-FDG PET-MRI of the hand in rheumatoid arthritis: initial results. Clin Rheumatol 2011;30:1247-50.
53. Moher D, Liberati A, Tetzlaff J, Altman DG, the PRISMA Group. Preferred reporting items for systematic reviews and meta-analyses: the PRISMA statement. PLoS Med 2009;6:e1000097.

Supporting information

Supplementary Appendix A: search strategies

Search	Topic
PubMed (MEDLINE): last search at 31 December 2012	
1	Disease: rheumatoid arthritis (RA), Juvenile Idiopathic Arthritis (JIA), Ankylosing Spondylitis (AS), Psoriatic Arthritis (PsA) or other Spondyloarthritis (SpA)
MeSH	((((("Arthritis, Rheumatoid"[Mesh:noexp])) OR ("Spondylarthropathies"[Mesh])) OR ("Arthritis, Juvenile Rheumatoid"[Mesh])) OR ("Synovitis"[Mesh:noexp])
	OR
Free text	((((((Bechterew[Title/Abstract]) OR (joint AND inflammation[Title/Abstract])) OR (synovi*[Title/Abstract])) OR (psoria*[Title/Abstract])) OR (arthrit*[Title/Abstract])) OR (ankylos*[Title/Abstract])) OR (rheum*[Title/Abstract])
2	Imaging Technique: Positron Emission Tomography
MeSH	tomography, emission-computed[mh]
	OR
Free text	(pet[tiab] OR pet/*[tiab] OR petscan*[tiab] OR (emission[tiab] AND (tomograph [tiab] OR tomographs [tiab] OR tomographic*[tiab] OR tomography[tiab] OR tomographies[tiab])))
	NOT
MeSH	(animals[mh] NOT humans[mh])
3	Combination
	#1 AND #2
Embase: last search at 31 December 2012	
1	'rheumatoid arthritis'/de OR 'ankylosing spondylitis'/exp OR 'juvenile rheumatoid arthritis'/exp OR 'psoriatic arthritis'/exp OR 'synovitis'/de
2	(joint AND inflammation:ab,ti) OR synovi*:ab,ti OR psoria*:ab,ti OR arthrit*:ab,ti OR ankylos*:ab,ti OR rheum*:ab,ti OR bechterew:ab,ti
3	'positron emission tomography'/exp OR 'tomography'/de
4	pet:ab,ti OR petscan*:ab,ti OR (emission AND tomograph:ab,ti) OR tomographs:ab,ti OR tomographic*:ab,ti OR tomographies:ab,ti
5	#1 OR #2
6	#3 OR #4
7	#5 AND #6
Cochrane Library; last search: 31 December 2012	
1	((((("Arthritis, Rheumatoid"[Mesh:noexp])) OR ("Spondylarthropathies"[Mesh])) OR ("Arthritis, Juvenile Rheumatoid"[Mesh])) OR ("Synovitis"[Mesh:noexp])
2	(Joint):ti,ab,kw and (Inflammation):ti,ab,kw OR (Bechterew):ti,ab,kw OR (synovi*):ti,ab,kw OR (psoria*):ti,ab,kw OR (arthrit*):ti,ab,kw OR (ankylos*):ti,ab,kw OR (rheum*):ti,ab,kw
3	"MeSH descriptor Positron-Emission Tomography, this term only
4	(pet):ti,ab,kw OR (pet/*):ti,ab,kw OR (petscan*):ti,ab,kw OR (emission):ti,ab,kw and (tomograph):ti,ab,kw OR (tomographs):ti,ab,kw OR (tomographic*):ti,ab,kw OR (tomography):ti,ab,kw OR (tomographies):ti,ab,kw
5	#1 OR #2
6	#3 OR #4
7	#5 AND #6

:ti,ab,kw = title and/or abstract and/or keywords; /de = descriptor, EMTree-term not

exploded; /exp = EMTree term exploded

Supplementary Appendix B: additional extracted PET data

Author (ref)	Image acquisition				Image reconstruction
	Scanner	FOV	p.i.(min)	dose	
Palmer et al (10)	Scanditronix PC 4096 (GE)	1	75±19	333±61 MBq	FPB (6.5mm)
Danfors et al (22)	GE 4096 (GE)	1	0	405-880 MBq	summation image
Roivainen et al (23)	Advance (GE)	1	0	358-377 MBq 424-440 MBq	OSEM (5mm)
Beckers et al (11)	UGM Penn PET 240 H	1	73 (51-100)	4 MBq/kg	OSEM (5.5mm)
Beckers et al (18)	UGM Penn PET 240 H	1	93±17	4 MBq/kg	OSEM (5.5mm)
Goerres et al (16)	Advance (GE)	WB	x	370 MBq	OSEM
Elzinga et al (19)	ECAT EXACT HR+ (Cti/Siemens)	1	60	370 or 455 MBq	FBP Hanning (7mm)
Laken et al (24)	ECAT EXACT HR+ (Cti/Siemens)	21 frames	40-60?	416±67 MBq	FBP Hanning + OSEM
Kubota K et al (12)	Biograph 16 siemens	WB	60	370 MBq	OSEM
Sato et al. (38)	ECAT EXACT 47 (Cti/Siemens)	WB	60	3 MBq/kg	OSEM
Taniguchi et al (20)	Discovery STE (GE)	WB	60	3.5 MBq/kg	OSEM
Tatheisi et al (13)	SET 2400 shimadzu	WB	60	34-228 MBq	OSEM
Elzinga et al (39)	ECAT EXACT HR+ (Cti/Siemens)	1	0	382±44 MBq	FBP Hanning (7mm)
Gent et al (37)	ECAT HRRT (Cti/Siemens)	1	10	457±51 MBq	OSEM
Okabe et al (21)	PET: SET 2400, Shimadzu PET/CT: Aquiduo, Toshiba	WB/TB	60	2.5-5.0 MBq/kg	FWHM 5mm
Okamura et al (14)	Biograph 16 Siemens	TB	60	5 MBq/kg	OSEM
Roivainen et al (17)	Discovery VCT (GE)	WB	45	255±22 MBq	FWHM 5.12 mm; OSEM
Vijayant et al (15)	Advance (GE)	WB	60	10 mCi	OSEM

FOV=field of view; p.i.=post-injection; min=minutes; GE=general electric; MBq(/kg)=Megabecquerel (per kilogram); FPB=filtered back projection; mm=millimeter; OSEM=ordered-subsets expectation-maximization; WB=whole body (e.g. shoulders to knees); FWHM=full with half maximum; mCi=microcurie

Supplementary Appendix C: tracers used for imaging inflammatory arthritis.

Tracer full name	abbreviation	Cellular target	Studies
fluorine-18- fluoro-deoxy-glucose	^{18}F-FDG	Metabolically active cells	10-21; 38;39
C^{11} (S-(+)-(d)-D-deprenyl	^{11}C-D-deprenyl	Unkown targeting mechanism	22
methyl-^{11}C-choline	^{11}C-choline	Synthesis of phospholipids in cell-membranes reflecting proliferative changes of tissues	23
^{11}C-(*R*)-PK11195	^{11}C-(*R*)-PK11195	Peripheral benzodiazepine receptors (PBRs), predominantly expressed on activated macrophages.	24; 37